

\*\*\*\*\*Newcastle University EPRINT version\*\*\*\*\*  
\*\*\*\*\*Originally presented at PEMD 2018 - will be available on IEEE Xplore late 2018\*\*\*\*\*  
\*\*\*\*\*The 9th International Conference on Power Electronics, Machines and Drives (IET)\*\*\*\*\*

# A Flux Concentrated Doubly Salient Linear Permanent Magnet Machine

*A. A. Almoraya, Student Member, IEEE \*, N. J. Baker\*, K. J. Smith\*, M. A. H. Raihan\**

*\*Electrical Power Research Group, School of Electrical and Electronic Engineering  
Newcastle University, Newcastle upon Tyne, NE17RU, UK, a.a.a.almoraya@ncl.ac.uk*

**Keywords:** V-shaped; linear vernier hybrid PM; power factor.

## Abstract

Different topologies of Vernier permanent magnet (PM) machines have been proposed for direct drive wave energy applications due to their high thrust and power density. However, this type of machine can suffer from low power factor (PF). In this paper, a flux concentrated doubly salient linear permanent magnet machine with V-shape PM arrays is proposed and compared to a consequent pole type machine. Using the configuration of V-shaped PMs allows the flux to be concentrated in iron spacers located between two pieces of PMs. This feature is shown to result in an improvement of the airgap flux density, which allows a reduction in electrical loading and hence an improvement in power factor.

In order to achieve a fair comparison, two doubly salient linear permanent magnet (DSLPM) machines with different PM configurations have been analysed and compared using transient FEA. The investigated machines have the same overall machine and, crucially, magnet volume. The results confirm that the proposed V-shape machine is capable of higher thrust force, higher no-load back EMF and can achieve a higher PF of 42% compared to the consequent pole machine, while it consumes the same amount of the PM material.

## 1 Introduction

Vernier permanent magnet (VPM) machines have been investigated and shown to be capable of torque and power density at low speed operation [1]. Using such type of machines in slow speed direct drive applications can contribute to a significant reduction in active electrical machine size without sacrificing the machine performance. In addition, due to the approximate sinusoidal back EMF waveforms, VPM machines can produce lower cogging torque compared with conventional PM machines. A linear version of the Vernier PM machine has been proposed for direct drive wave energy converters offering high shear stress[2, 3]. However, direct drive machines including Vernier PM machines, variable reluctance machines and transverse flux PM machines tend to suffer from low PF, typically less than 0.4 [1]. For a fixed real power output, the capacity and relative cost of the converter is inversely proportional to the power factor of the electrical machine[4]. Therefore, power factor improvement of Vernier machines is a vital goal for machine designers in the field of wave energy converters.

In literature, different topologies have been proposed to improve the PF. One such method, involving an auxiliary DC winding was employed in [1] which naturally leads to an increase in copper loss, converter loss and material cost. In addition, its PMs are located on the translator resulting in poor magnet utilisation for linear machines with a large amplitude of oscillation. In [4], the authors proposed an effective topology of a rotary Vernier machine with an improved power factor. Again, converting this machine into linear version requires a large amount of PM material since the PMs are located in the translator,

The Consequent Pole (CP) machines have been nominated as an economic alternative design of the baseline machines where 50% of PM material can be saved without sacrificing the machine performance [5, 6]. In this study, the CP machine shown in Figure 1 (a) is used as a baseline machine to assess the possibility of improving the machine performance without increasing the magnet mass.

The object of this paper is to propose a doubly salient linear PM machine which adopts V-shape PM arrangement without iron ribs, as shown for a rotary version in [7]. The use of conventional V-shaped PM arrays in rotary Vernier machines has been proposed in [8, 9], while the linear version has not been reported elsewhere. The key feature of the proposed machine is that the magnets are placed in the stationary part of the machine contributing to a better magnet utilization. It is shown that by implementing the new structure, the airgap flux density from PMs can be improved resulting in a lower electric loading for a given force and hence an improved power factor.

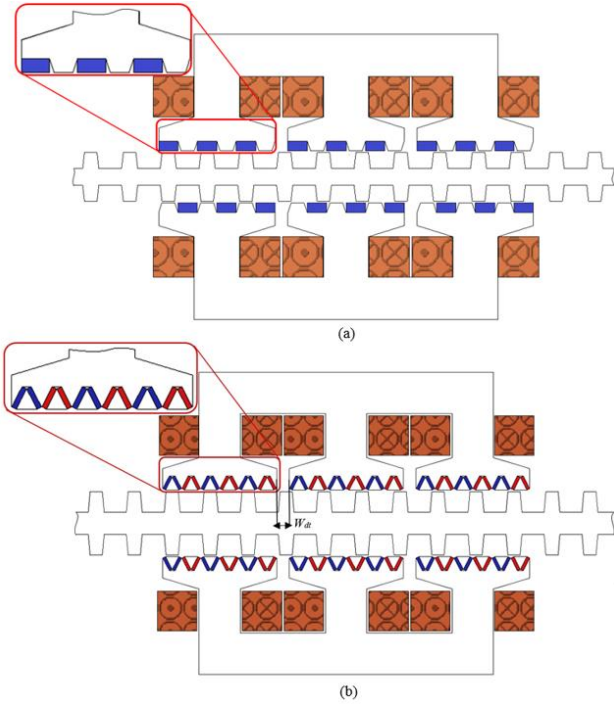


Fig.1 Machine configuration (a) consequent pole machine and (b) proposed V-shaped machine

sandwiched between two stators.

In order to obtain a three phase machine the mechanical displacement  $W_{dt}$  between the adjacent teeth should be 120 electrical degrees apart, and that can be achieved by making this space satisfy (1),

where  $n$  is a positive integer and  $\tau_1$  is the mover pitch.

The proposed machine employs a V-shaped PM array without iron ribs. The key features of this topology is that the V-shaped PM array concentrates the flux in the pole area leading to a significant improvement of the airgap flux density. The removal of the steel ribs located around the magnets' edges would contribute to a noticeable reduction in the leakage flux. In addition, by removing these ribs the  $q$ -axes airgap length is increased, and hence the  $L_q$  is reduced.

### 3 Operation principle

The proposed V-shape machine operates upon the same principle as the CP machine. The proposed machine also adopts the magnetic gearing effect, meaning a small translator displacement produces a rapid flux linkage change. As it can be seen in Fig.2 the flux distribution in the stator varies 120 electrical degrees while the translator moves only 8mm, which is equivalent to 1/3 of the translator pole pitch. When the translator is at its initial position,  $x=0$  (the alignment position for phase one), the coil flux linkage reaches its negative peak value, while the no-load back EMF is zero. As the translator moves  $1/4$  of the translator pole pitch, coil flux linkage is zero, while the no-load back EMF achieves its positive maximum. Again, when the translator moves further by  $1/2$  pole pitch from its initial position, the polarity of the coil flux linkage is reversed and achieves its maximum positive, whereas the no-load back EMF is zero. As the translator moves  $3/4$  of the translator pole pitch, the coil flux linkage is zero, while the back EMF is negative maximum. Thus, the flux linkage polarity is rapidly changed over a small translator movement, contributing to the high thrust force density.

$$W_{dt} = (n \pm 1/3)\tau_1 \quad \text{or} \quad (n \pm 1/6)\tau_1$$

### 4 Machine optimization

In order to obtain a fair comparison between the two machines the key parameters are kept the same in both machines. These include the machine volume, rated speed and current density. The pole pitch and magnet volume are also fixed in the proposed

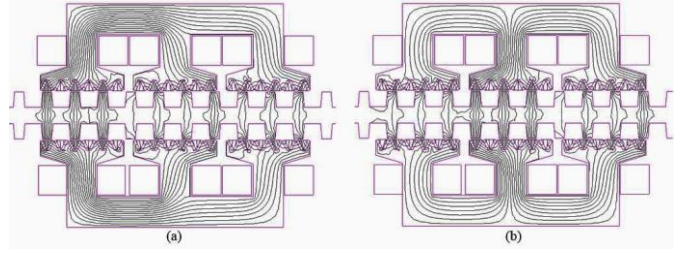


Fig.2 No-load field distribution (a)  $x=0$ , (b)  $x=1/3\tau_1$

The description of the proposed machine configuration and operation principle is presented in section 2 and section 3 respectively. Section 4 introduces the machine optimisation which includes the effect of varying the magnet dimensions and airgap length on the thrust force, no-load back EMF and cogging force. Section 5 compares the electromagnetic and electrical performances for the consequent pole (CP) machine and the proposed machine assessed by FEA. Finally, the conclusion is given in section 6.

### 2 Description of the proposed topology

The structure of the proposed three phase machine is shown in Figure 1 (b). It has a symmetric double-sided stator with E-shaped iron cores facing each other. Each phase consists of two coils which are individually wound around each stator tooth and connected in series. The 12 PMs in a V-shape arrangement are mounted in each stator tooth. The translator is formed of salient teeth and is

V-shape machine as the magnet V-angle ( $\alpha$ ) and magnet dimensions were optimised based on these constraints. The optimization of the magnet thickness, magnet width and V-angle (identified in Figure 3) is conducted in this section to achieve the optimum thrust force. Four designs shown in Figure 4 have been analysed and force has been calculated for different cases as summarised in Table 1. From the obtained results it can be seen that the highest thrust force can be achieved by choosing design 1, which was therefore selected.

The effect of varying the airgap length on the thrust force and power factor was analyzed and compared. Figure 5 illustrates the variation of the thrust force and power factor with respect to the airgap length for the proposed design. It can be found that both thrust force and power factor drop as the airgap length increases. However, the small airgap length may significantly increase the mechanical and assembly complexity, and hence the reliability of the machine might be affected [10, 11]. Therefore, the airgap length is selected to be 1 mm.

## 5 Machine analysis and performance comparison

Based on the FEA the steady-state and transient performances of the CP and proposed V-shape machines are analyzed and compared. The main parameters for both designs are listed in Table 2.

### 5.1 Airgap flux density

Both simulated machines operate by modulating the PM field modulation by translator teeth. Therefore, analyzing the no-load airgap flux density distribution is a good way of comparing performance. Figure 6 shows the airgap flux density distribution along the airgap. It can be seen in this figure the maximum airgap flux density for the proposed and CP machines are 1.65 T and 1.18 T respectively. Hence, the proposed V-shape machine possesses the highest airgap flux density which benefits from the flux concentration of the V-shape PM array.

Figure 7 illustrates a comparison of the plotted no-load field distributions predicted by FEA. From Figure 7 (a) it can be observed that the flux leakage is quite high in the CP machine. On the other hand, the flux leakage of the proposed machine is noticeably reduced as shown in Figure 7 (b). Although the CP machine adopts the consequent pole structure which contributes to a significant reduction of the leakage flux and leads to a major increase in the main flux as presented in [5, 10, 11], the V-shaped machine is still capable of reducing the leakage flux further. This structure effectively directs the flux produced by PMs towards the stator windings. Therefore, the proposed V-shape machine possesses higher main flux and lower leakage flux compared with its counterpart.

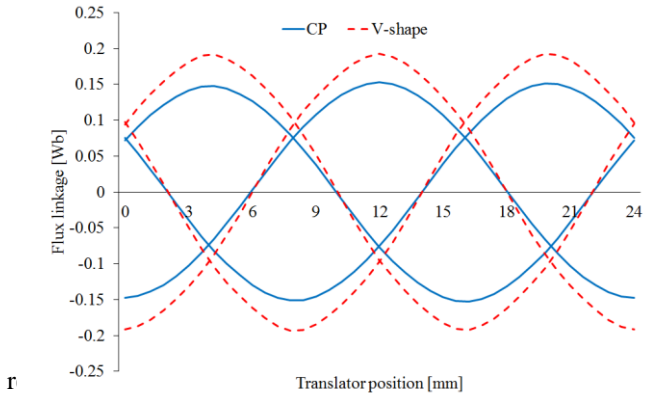


Fig.8 No-load flux linkage waveforms for both designs

Parameter	CP	V-shape
Number of phases	3	
Translator pole pitch [mm]	24	
Pole pitch [mm]	12	
Airgap length [mm]	1	
Stack length[mm]	50	
Number of turns/coil	90	
Translator tooth height [mm]	10	
Machine active length [mm]	232	
Stator tooth width [mm]	72	
Magnet remanence [T]	1.24	
Active PM volume [cm <sup>3</sup> ]	64.8	
Rated speed [m/s]	1.2	
Magnet width [mm]	12	9
Magnet thickness [mm]	6	2
Number of the total PMs	18	72

Table 2: Key parameters for both CP and proposed V-shape machines

## 5.2 No-load flux linkage and back EMF

In order to assess the validity of the comparison between the same: rated speed, number of turns of the armature per phase, no-load flux linkage for the CP and proposed machine. It can linkage than that of the CP machine, and this is due the fact tha the CP machine. The induced no-load back EMF for both mac be seen that the proposed V-shape machine produces the pe machine. Which means, the proposed machine produces 22.6% utilizing the same magnet mass. However, it can be also observ design are more sinusoidal than that of the proposed design. T EMF in the proposed machine have increased as shown in Fig. of the iron ribs.

## 5.3 Thrust force capability

Figure 10 shows the thrust force waveforms for the CP and proposed machines with the same rated armature current. The applied current is assumed to be sinusoidal and is fed in phase with the no-load back EMF. It can be seen that by employing the V-shape topology the average values of the thrust force of the V-shape and CP machines are 880 N and 750 N respectively, meaning that the new machine offers 14.8% extra force with the same electrical loading. It should be also indicated that the force ripple of the V-shape machine is 9% of its thrust force, which is 3.4% higher than that of the CP machine. This is due to the fact that the no-load back EMF waveforms of the CP machine are more sinusoidal. In this publication, the force ripple is defined as the ratio of the peak to peak force to the average force. This is defined as:

$$\Delta F = (F_{max} - F_{min}) / F_{avg} \quad (2)$$

where  $F_{max}$ ,  $F_{min}$  and  $F_{avg}$  are the maximum value, minimum value and average value of the thrust force. Fig.11 shows the thrust force characteristics of the CP and proposed V-shape machine. It can be seen that for both machines the thrust force-

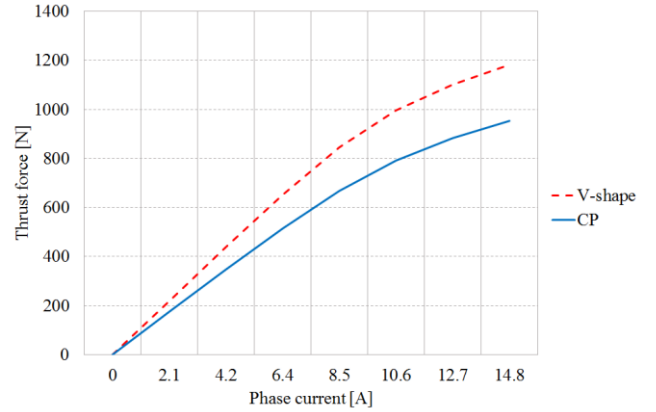


Fig.11 Overloading force capability for both machines

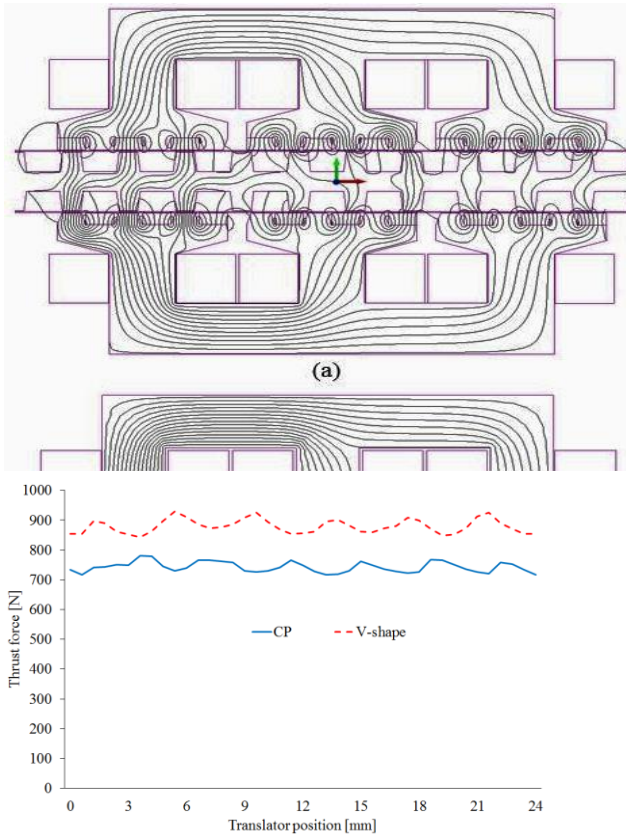


Figure10 Thrust force waveforms for both designs

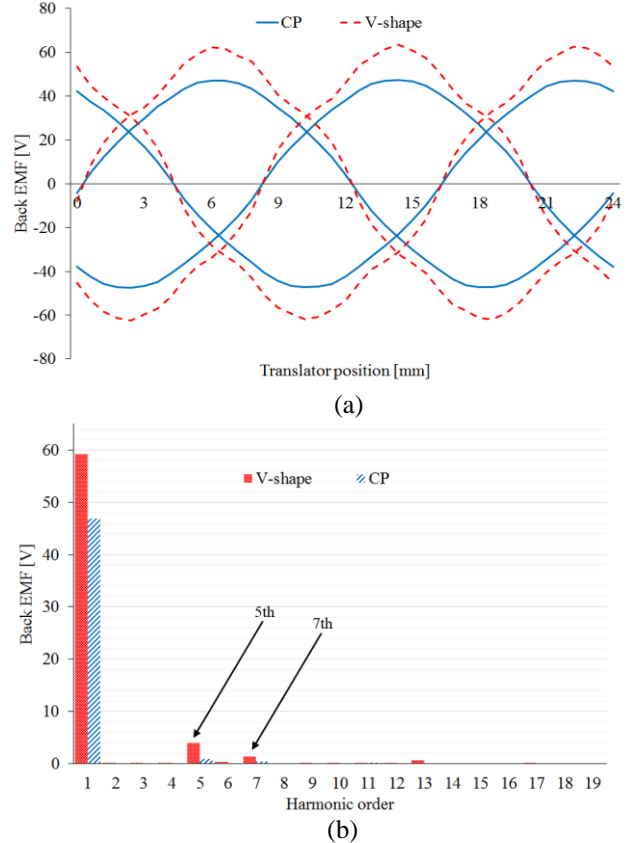


Figure .9 (a) No-load back EMF waveforms for both designs (b) harmonics



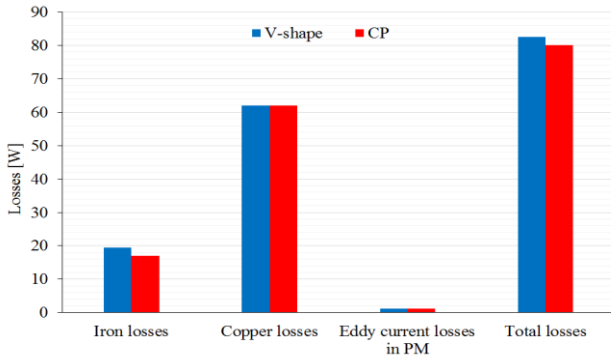


Fig.13 Comparison of losses

current relationship is almost linear below the rated value of the armature current, after which the increase of the thrust force for both machines is non-linear due to magnetic saturation. However, the proposed V-shape machine is able to deliver higher force at various load conditions than that of the CP machine. Moreover, the cost effectiveness is assessed in terms of the thrust force production of both machines. The average thrust per volume for both machines is calculated according to (3). It can be observed that the thrust force density of the proposed V-shape machine is about  $43.2 \times 10^4 \text{ N/m}^3$ , while the thrust force density of the CP machine is nearly  $36.7 \times 10^4 \text{ N/m}^3$ . Which means, the proposed V-shape machine can offer 15% higher thrust force density compared to the CP machine.

$$F_d = F/V_m \quad (3)$$

Where  $F_d$  is the force density,  $F$  is the thrust force and  $V_m$  is the machine volume. Moreover, shear stress which is defined as the thrust force per active airgap area is also calculated for both V-shape and CP machines. By applying (4) the shear stress of  $74 \text{ kN/m}^2$  and  $63.8 \text{ kN/m}^2$  can be achieved by the proposed V-shape and CP machines respectively.

$$F_{sh} = F/A_a \quad (4)$$

#### 5.4 Cogging force

Cogging force is a common phenomenon in PM machines caused by the magnetic attraction between stator PMs and translator teeth, which may lead to mechanical vibration and acoustic noise. Therefore, minimizing cogging force is a vital requirement for PM machine design. The cogging force waveforms for both the CP and proposed machines are plotted and compared in Figure 12. It can be found that the peak to peak cogging force of the proposed V-shape and CP machine are  $80.8 \text{ N}$  and  $62 \text{ N}$  respectively. Which means, the V-shaped machine produces 23.3% higher cogging force than that of the CP one. This is due to the removal of the iron ribs in the proposed machine which caused an increase of 6% in the THD of the back EMF[7]. Moreover, the adoption of the tapered ferromagnetic poles in the CP machine can contribute to a reduction in the cogging force [5, 11]. However, both V-shape and CP machines have acceptable levels of the cogging force which represent only 9% and 8% with respect to the average force respectively.

#### 5.5 Losses and efficiency

The losses and efficiency for the CP and proposed V-shape machines are estimated. In this paper, only the electromagnetic losses for both design were investigated. Therefore, the copper losses can be expressed as:

$$P_{Cu} = m \cdot R_{ph} \cdot I_{rms}^2 \quad (5)$$

where  $m$  is the number of phases,  $R_{ph}$  is the phase resistance and  $I_{rms}$  is the armature current in RMS value.

Therefore, the efficiency is

$$\eta = P_{out} / (P_{out} + P_{Cu} + P_{iron}) \quad (6)$$

where  $P_{out}$ ,  $P_{Cu}$ , and  $P_{iron}$  are the output power, copper loss, and iron loss, respectively. Figure 13 compares the losses of the both machines which is obtained using the above equations. The efficiency of the proposed V-shape machine is 92.5%, while the efficiency of the CP machine is 91.7%.

## 6 Conclusion

In this paper, a new version of the linear doubly salient machine structure is proposed. The V-shaped PM arrays are utilised in the proposed machine which allow the flux concentration phenomenon to be exploited. By using FEA two doubly salient linear PM machines have been designed, investigated and compared based on the same key parameters including magnet mass and current density. The simulation results are concluded that the proposed V-shape machine:

- is capable of higher no-load back EMF, thrust force and power factor compared with CP machine with the percentage of 22.6%, 14.8% and 42% respectively.
- offers the best thrust force capability.
- possesses 6% higher THD in the no-load back EMFs, and thus produces 23.3% higher cogging force and 3.4% force ripple compared with CP machine. However, the cogging force of the proposed machine is only 9% of its average thrust force.

## References

- [1] T. W. Ching, K. T. Chau, and W. Li, "Power factor improvement of a linear vernier permanent-magnet machine using auxiliary dc field excitation," *IEEE Transactions on Magnetics*, vol. 52, pp. 1-4, 2016.
- [2] P. R. M. Brooking and M. A. Mueller, "Power conditioning of the output from a linear vernier hybrid permanent magnet generator for use in direct drive wave energy converters," *IEE Proceedings-Generation, Transmission and Distribution*, vol. 152, pp. 673-681, 2005.
- [3] M. A. Mueller and N. J. Baker, "Modelling the performance of the vernier hybrid machine," *IEE Proceedings-Electric Power Applications*, vol. 150, pp. 647-654, 2003.
- [4] D. Li, R. Qu, and T. A. Lipo, "High-power-factor vernier permanent-magnet machines," *IEEE Transactions on Industry Applications*, vol. 50, pp. 3664-3674, 2014.
- [5] A. A. Almoraya, N. J. Baker, K. J. Smith, and M. A. H. Raihan, "Development of a double-sided consequent pole linear vernier hybrid permanent-magnet machine for wave energy converters," in *Electric Machines and Drives Conference (IEMDC), 2017 IEEE International*, 2017, pp. 1-7.
- [6] Y. Gao, R. Qu, D. Li, J. Li, and G. Zhou, "Consequent-pole flux-reversal permanent-magnet machine for electric vehicle propulsion," *IEEE Transactions on Applied Superconductivity*, vol. 26, pp. 1-5, 2016.
- [7] S. Yang, N. J. Baker, B. C. Mecrow, C. Hilton, G. Sooriyakumar, D. Kostic-Perovic, *et al.*, "Cost reduction of a permanent magnet in-wheel electric vehicle traction motor," in *Electrical Machines (ICEM), 2014 International Conference on*, 2014, pp. 443-449.
- [8] L. Xu, G. Liu, W. Zhao, and J. Ji, "Hybrid Excited Vernier Machines with All Excitation Sources on the Stator for Electric Vehicles," *Progress In Electromagnetics Research M*, vol. 46, pp. 113-123, 2016.
- [9] G. Xu, L. Jian, W. Gong, and W. Zhao, "Quantitative comparison of flux-modulated interior permanent magnet machines with distributed windings and concentrated windings," *Progress In Electromagnetics Research*, vol. 129, pp. 109-123, 2012.
- [10] D. Li, R. Qu, J. Li, and W. Xu, "Consequent-pole toroidal-winding outer-rotor vernier permanent-magnet machines," *IEEE Transactions on Industry Applications*, vol. 51, pp. 4470-4481, 2015.
- [11] A. A. Almoraya, N. J. Baker, K. J. Smith, and M. A. H. Raihan, "An investigation of a linear flux switching machine with tapered ferromagnetic poles," in *Electrical Machines and Systems (ICEMS), 2017 20th International Conference on*, 2017, pp. 1-5.